

Chapter 6

Solution of Navier-Stokes Equations for Incompressible Flows Using SIMPLE and MAC Algorithms

6.1 Introduction

In Cartesian coordinates, the governing equations for incompressible three-dimensional flows are

$$\frac{\partial u}{\partial x} + \frac{\partial v}{\partial y} + \frac{\partial w}{\partial z} = 0 \quad (6.1)$$

$$\frac{\partial u}{\partial t} + \frac{\partial(u^2)}{\partial x} + \frac{\partial(uv)}{\partial y} + \frac{\partial(uw)}{\partial z} = -\frac{\partial p}{\partial x} + \frac{1}{Re} \left[\frac{\partial^2 u}{\partial x^2} + \frac{\partial^2 u}{\partial y^2} + \frac{\partial^2 u}{\partial z^2} \right] \quad (6.2)$$

$$\frac{\partial v}{\partial t} + \frac{\partial(uv)}{\partial x} + \frac{\partial(v^2)}{\partial y} + \frac{\partial(vw)}{\partial z} = -\frac{\partial p}{\partial y} + \frac{1}{Re} \left[\frac{\partial^2 v}{\partial x^2} + \frac{\partial^2 v}{\partial y^2} + \frac{\partial^2 v}{\partial z^2} \right] \quad (6.3)$$

$$\frac{\partial w}{\partial t} + \frac{\partial(uw)}{\partial x} + \frac{\partial(vw)}{\partial y} + \frac{\partial(w^2)}{\partial z} = -\frac{\partial p}{\partial z} + \frac{1}{Re} \left[\frac{\partial^2 w}{\partial x^2} + \frac{\partial^2 w}{\partial y^2} + \frac{\partial^2 w}{\partial z^2} \right] \quad (6.4)$$

In this chapter no assumption is made about the relative magnitude of the velocity components, consequently the full forms of the Navier-Stokes equations are solved. Methods described in this section will be based, basically, on finite-volume and finite-difference discretizations and on the solution of a Poisson

equation to determine the pressure. It may be mentioned that these methods use primitive variables u , v , w and p as function of x , y , z , t and Re which are preferable in flow calculations.

6.2 Staggered Grid

As it has been seen, the major difficulty encountered during solution of incompressible flow is the non-availability of any obvious equation for the pressure. This difficulty can be resolved in the stream- function-vorticity approach. This approach loses its advantage when three-dimensional flow is computed because of the fact that a single scalar stream-function does not exist in three-dimensional space. A three-dimensional problem demands a primitive-variable approach. Efforts have been made so that two-dimensional as well as three-dimensional problems could be computed following a primitive variable approach without encountering non-physical wiggles in the pressure distribution. As a remedy, it has been suggested to employ a different grid for each of the dependent variables.

Such a staggered grid for the dependant variables in a flow field was first used by Harlow and Welch (1965), in their very well known MAC (Marker and Cell) method. Since then, it has been used by many researchers. Specifically, SIMPLE (Semi Implicit Method for Pressure Linked Equations) procedure of Patankar and Spalding (1972) has become popular. Figure 6.1 shows a two-dimensional staggered where independent variables ($u_{i,j}$, $v_{i,j}$ and $p_{i,j}$) with the same indices staggered to one another. Extension to three-dimensions is straight-forward. The computational domain is divided into a number of cells, which are shown as “main control volume” in Fig. 6.1. The location of the velocity components are at the center of the cell faces to which they are normal. If a uniform grid is used, the locations are exactly at the midway between the grid points. In such cases the pressure difference between the two adjacent cells is the driving force for the velocity component located at the interface of these cells. The finite-difference approximation is now physically meaningful and the pressure field will accept a reasonable pressure distribution for a correct velocity field.

Another important advantage is that transport rates across the faces of the control volumes can be computed without interpolation of velocity components. The detailed outline of the two different solution procedures for the full Navier-Stokes equations with primitive variables using staggered grid will be discussed in subsequent sections. First we shall discuss the SIMPLE algorithm and then the MAC method will be described.

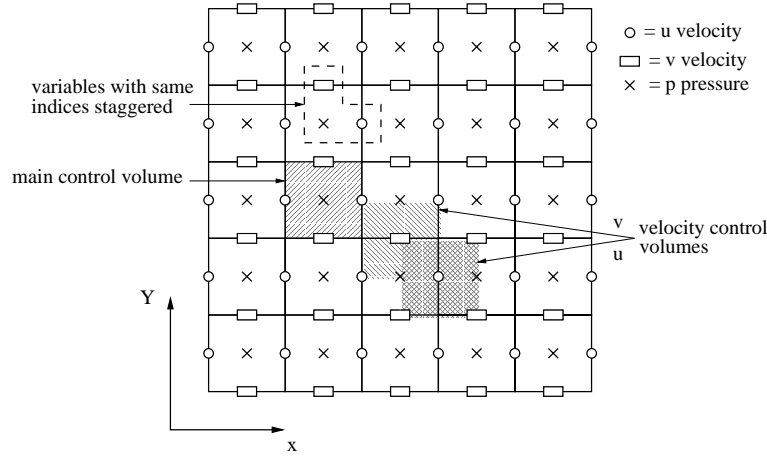


Figure 6.1: Staggered grid.

6.3 Semi Implicit Method for Pressure Linked Equations (SIMPLE)

SIMPLE algorithm is based on finite-volume discretization of the Navier-Stokes equations. The method was introduced by Patankar and Spalding (1972). The discretization indicated below corresponds to a uniform grid. The more general case of a non-uniform grid can be obtained from Patankar (1980). Consider the continuity equation

$$\frac{\partial u}{\partial x} + \frac{\partial v}{\partial y} = 0$$

For the control volume shown in Fig. 6.2. The application of the finite-volume method to the continuity equation produces the following discretized form of the equation

$$(u_{i,j}^{n+1} - u_{i-1,j}^{n+1}) \Delta y + (v_{i,j}^{n+1} - v_{i,j-1}^{n+1}) \Delta x = 0 \quad (6.5)$$

6.3.1 x - momentum equation

The Navier-Stokes equation in x -direction in conservative form (using continuity equation) is given as

$$\frac{\partial u}{\partial t} + \frac{\partial(u^2)}{\partial x} + \frac{\partial(uv)}{\partial y} + \frac{\partial p}{\partial x} = \frac{1}{Re} \left[\frac{\partial^2 u}{\partial x^2} + \frac{\partial^2 u}{\partial y^2} \right]$$

6.4 Computational Fluid Dynamics

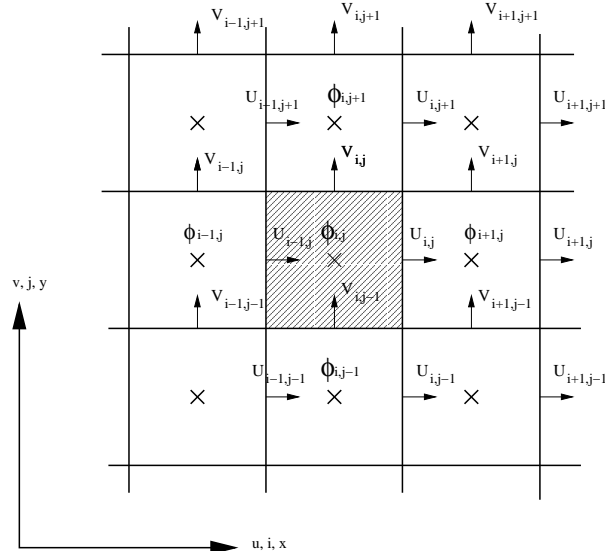


Figure 6.2: Control volume for continuity equation.

Integrating over the u -control volume (Fig. 6.3), we can write

$$\begin{aligned} & \frac{\Delta x \Delta y}{\Delta t} (u_{i,j}^{n+1} - u_{i,j}^n) + \iint \left[\frac{\partial}{\partial x} \left\{ u^2 - \frac{1}{Re} \frac{\partial u}{\partial x} \right\} + \frac{\partial}{\partial y} \left\{ uv - \frac{1}{Re} \frac{\partial u}{\partial y} \right\} \right] dx dy \\ & + \iint \left(\frac{\partial p}{\partial x} \right) dx dy = 0 \end{aligned}$$

Application of Green's theorem to the above expression leads to

$$\begin{aligned} & \frac{\Delta x \Delta y}{\Delta t} (u_{i,j}^{n+1} - u_{i,j}^n) + \left(E_{i+\frac{1}{2},j}^1 - E_{i-\frac{1}{2},j}^1 \right) \Delta y + \left(F_{i,j+\frac{1}{2}}^1 - F_{i,j-\frac{1}{2}}^1 \right) \Delta x \\ & + (p_{i+1,j}^{n+1} - p_{i,j}^{n+1}) \Delta y = 0 \end{aligned} \quad (6.6)$$

where E^1 and F^1 are defined as

$$E^1 = u^2 - \frac{1}{Re} \frac{\partial u}{\partial x}$$

and

$$F^1 = uv - \frac{1}{Re} \frac{\partial u}{\partial y}$$

E^1 and F^1 are axial and transverse fluxes of x -momentum. Thus

$$E_{i+\frac{1}{2},j}^1 = 0.25 (u_{i,j} + u_{i+1,j})^2 - \frac{1}{Re} \frac{(u_{i+1,j} - u_{i,j})}{\Delta x}$$

$$E_{i-\frac{1}{2},j}^1 = 0.25 (u_{i-1,j} + u_{i,j})^2 - \frac{1}{Re} \frac{(u_{i,j} - u_{i-1,j})}{\Delta x}$$

$$F_{i,j+\frac{1}{2}}^1 = 0.25(v_{i,j} + v_{i+1,j})(u_{i,j} + u_{i,j+1}) - \frac{1}{Re} \left(\frac{u_{i,j+1} - u_{i,j}}{\Delta y} \right)$$

$$F_{i,j-\frac{1}{2}}^1 = 0.25 (v_{i,j-1} + v_{i+1,j-1}) (u_{i,j-1} + u_{i,j}) - \frac{1}{Re} \left(\frac{u_{i,j} - u_{i,j-1}}{\Delta y} \right)$$

The linearized form of these equations are

$$E_{i+\frac{1}{2},j}^1 = 0.25 \left(u_{i,j}^n + u_{i+1,j}^n \right) \left(u_{i,j}^{n+1} + u_{i+1,j}^{n+1} \right) - \frac{1}{Re} \frac{\left(u_{i+1,j}^{n+1} - u_{i,j}^{n+1} \right)}{\Delta x}$$

$$E_{i-\frac{1}{2},j}^1 = 0.25 \left(u_{i-1,j}^n + u_{i,j}^n \right) \left(u_{i-1,j}^{n+1} + u_{i,j}^{n+1} \right) - \frac{1}{Re} \frac{\left(u_{i,j}^{n+1} - u_{i-1,j}^{n+1} \right)}{\Delta x}$$

$$F_{i,j+\frac{1}{2}}^1 = 0.25 \left(v_{i,j}^n + v_{i+1,j}^n \right) \left(u_{i,j}^{n+1} + u_{i,j+1}^{n+1} \right) - \frac{1}{Re} \frac{\left(u_{i,j+1}^{n+1} - u_{i,j}^{n+1} \right)}{\Delta y}$$

$$F_{i,j-\frac{1}{2}}^1 = 0.25 \left(v_{i,j-1}^n + v_{i+1,j-1}^n \right) \left(u_{i,j-1}^{n+1} + u_{i,j}^{n+1} \right) - \frac{1}{Re} \frac{\left(u_{i,j}^{n+1} - u_{i,j-1}^{n+1} \right)}{\Delta y}$$

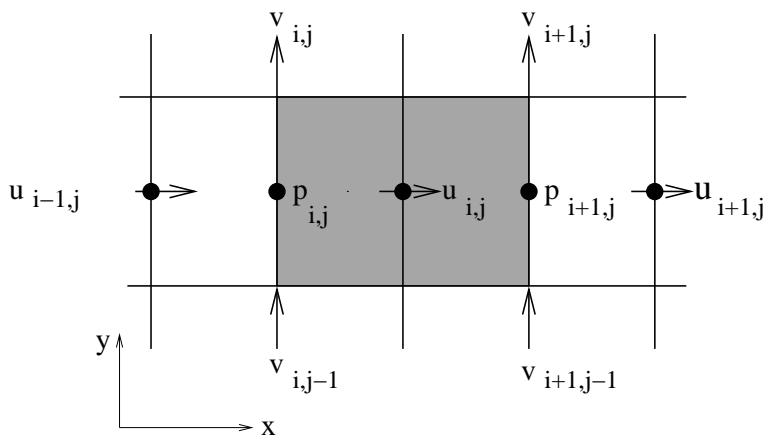


Figure 6.3: Control volume for x -momentum equation.

Consequently, eq. (6.6) can be written as

$$\left(\frac{\Delta x \Delta y}{\Delta t} + a_{i,j}^u\right) u_{i,j}^{n+1} + \sum a_{nb}^u u_{nb}^{n+1} + b^u + \Delta y (p_{i+1,j}^{n+1} - p_{i,j}^{n+1}) = 0 \quad (6.7)$$

6.6 Computational Fluid Dynamics

In the above equation, $\sum a_{nb}^u u_{nb}^{n+1}$ signifies all the convective and diffusive contributions from the neighboring nodes ($u_{i+1,j}^{n+1}, u_{i-1,j}^{n+1}, u_{i,j+1}^{n+1}, u_{i,j-1}^{n+1}$ and their coefficients). The coefficients $a_{i,j}^u$ and a_{nb}^u contain grid sizes, and the solution of u and v at n th time level. The term b^u equals $-\Delta x \Delta y u_{i,j}^n / \Delta t$. In the following sub-section, equation (6.6) has been written term by term so that $a_{i,j}^u, a_{nb}^u$ and b^u in equation (6.7) can be clearly determined.

Equation (6.6) can be expanded as

$$\begin{aligned} & \left(\frac{\Delta x \Delta y}{\Delta t} u_{i,j}^{n+1} - \frac{\Delta x \Delta y}{\Delta t} u_{i,j}^n \right) + \\ & u_{i,j}^{n+1} \left\{ 0.25(u_{i,j}^n + u_{i+1,j}^n) \Delta y + \frac{\Delta y}{Re \Delta x} \right\} + u_{i+1,j}^{n+1} \left\{ 0.25(u_{i,j}^n + u_{i+1,j}^n) \Delta y - \frac{\Delta y}{Re \Delta x} \right\} \\ & - u_{i,j}^{n+1} \left\{ 0.25(u_{i-1,j}^n + u_{i,j}^n) \Delta y - \frac{\Delta y}{Re \Delta x} \right\} - u_{i-1,j}^{n+1} \left\{ 0.25(u_{i-1,j}^n + u_{i,j}^n) \Delta y + \frac{\Delta y}{Re \Delta x} \right\} \\ & + u_{i,j}^{n+1} \left\{ 0.25(v_{i,j}^n + v_{i+1,j}^n) \Delta x + \frac{\Delta x}{Re \Delta y} \right\} + u_{i+1,j}^{n+1} \left\{ 0.25(v_{i,j}^n + v_{i+1,j}^n) \Delta x - \frac{\Delta x}{Re \Delta y} \right\} \\ & - u_{i,j}^{n+1} \left\{ 0.25(v_{i,j-1}^n + v_{i+1,j-1}^n) \Delta x - \frac{\Delta x}{Re \Delta y} \right\} - u_{i,j-1}^{n+1} \left\{ 0.25(v_{i,j-1}^n + v_{i+1,j-1}^n) \Delta x \right. \\ & \quad \left. + \frac{\Delta x}{Re \Delta y} \right\} + (p_{i+1,j}^{n+1} - p_{i,j}^{n+1}) \Delta y = 0 \end{aligned}$$

or,

$$\begin{aligned} & \left[\frac{\Delta x \Delta y}{\Delta t} + 0.25(u_{i,j}^n + u_{i+1,j}^n) \Delta y - 0.25(u_{i-1,j}^n + u_{i,j}^n) \Delta y + 0.25(v_{i,j}^n + v_{i+1,j}^n) \Delta x \right. \\ & \quad \left. - 0.25(v_{i,j-1}^n + v_{i+1,j-1}^n) \Delta x + \frac{\Delta y}{Re \Delta x} + \frac{\Delta y}{Re \Delta x} + \frac{\Delta x}{Re \Delta y} + \frac{\Delta x}{Re \Delta y} \right] u_{i,j}^{n+1} \\ & + u_{i+1,j}^{n+1} \left\{ 0.25(u_{i,j}^n + u_{i+1,j}^n) \Delta y - \frac{\Delta y}{Re \Delta x} \right\} + u_{i-1,j}^{n+1} \left\{ 0.25(u_{i-1,j}^n + u_{i,j}^n) \Delta y - \frac{\Delta y}{Re \Delta x} \right\} \\ & + u_{i,j+1}^{n+1} \left\{ 0.25(v_{i,j}^n + v_{i+1,j}^n) \Delta x - \frac{\Delta x}{Re \Delta y} \right\} + u_{i,j-1}^{n+1} \left\{ -0.25(v_{i,j-1}^n + v_{i+1,j-1}^n) \Delta x \right. \\ & \quad \left. - \frac{\Delta x}{Re \Delta y} \right\} - \frac{\Delta x \Delta y}{\Delta t} u_{i,j}^n + \Delta y (p_{i+1,j}^{n+1} - p_{i,j}^{n+1}) = 0 \end{aligned}$$

6.3.2 y- momentum equation

$$\frac{\partial v}{\partial t} + \frac{\partial}{\partial x}(uv) + \frac{\partial(v)^2}{\partial y} + \frac{\partial p}{\partial y} = \frac{1}{Re} \left\{ \frac{\partial^2 v}{\partial x^2} + \frac{\partial^2 v}{\partial y^2} \right\}$$

Using the control volume shown in Fig. 6.4, the y momentum equation can be integrated over v -control volume as

$$\begin{aligned} \frac{\Delta x \Delta y}{\Delta t} (v_{i,j}^{n+1} - v_{i,j}^n) + \iint \left[\frac{\partial}{\partial x} \left\{ uv - \frac{1}{Re} \frac{\partial v}{\partial x} \right\} + \frac{\partial}{\partial y} \left\{ v^2 - \frac{1}{Re} \frac{\partial v}{\partial y} \right\} \right] dx dy \\ + \iint \left(\frac{\partial p}{\partial y} \right) dx dy = 0 \end{aligned}$$

Application of Green's theorem to the above expression leads to

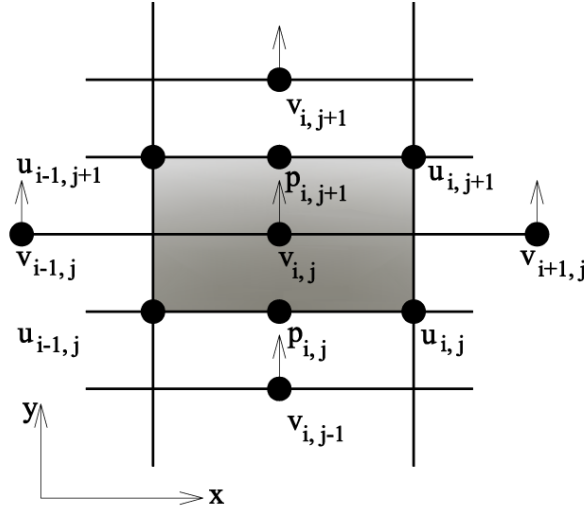


Figure 6.4: Control volume for y -momentum equation.

$$\begin{aligned} \frac{\Delta x \Delta y}{\Delta t} (v_{i,j}^{n+1} - v_{i,j}^n) + (E_{i+1/2,j}^2 - E_{i-1/2,j}^2) \Delta y + (F_{i,j+1/2}^2 - F_{i,j-1/2}^2) \Delta x \\ + (p_{i,j+1}^{n+1} - p_{i,j}^{n+1}) \Delta x = 0 \end{aligned} \quad (6.8)$$

$$E^2 = uv - \frac{1}{Re} \frac{\partial v}{\partial x}, \quad F^2 = v^2 - \frac{1}{Re} \frac{\partial v}{\partial y}$$

6.8 Computational Fluid Dynamics

Here E^2 and F^2 are the axial and transverse fluxes of y-momentum

$$E_{i+1/2,j}^2 = 0.25(u_{i,j} + u_{i,j+1})(v_{i,j} + v_{i+1,j}) - \frac{1}{Re} \frac{(v_{i+1,j} - v_{i,j})}{\Delta x}$$

$$E_{i-1/2,j}^2 = 0.25(u_{i-1,j} + u_{i-1,j+1})(v_{i-1,j} + v_{i,j}) - \frac{1}{Re} \frac{(v_{i,j} - v_{i-1,j})}{\Delta x}$$

$$F_{i,j+1/2}^2 = 0.25(v_{i,j} + v_{i,j+1})^2 - \frac{1}{Re} \frac{(v_{i,j+1} - v_{i,j})}{\Delta y}$$

$$F_{i,j-1/2}^2 = 0.25(v_{i,j-1} + v_{i,j})^2 - \frac{1}{Re} \frac{(v_{i,j} - v_{i,j-1})}{\Delta y}$$

The linearized form of these equations are

$$E_{i+\frac{1}{2},j}^2 = 0.25 (u_{i,j}^n + u_{i,j+1}^n) (v_{i,j}^{n+1} + v_{i+1,j}^{n+1}) - \frac{1}{Re} \frac{(v_{i+1,j}^{n+1} - v_{i,j}^{n+1})}{\Delta x}$$

$$E_{i-\frac{1}{2},j}^2 = 0.25 (u_{i-1,j}^n + u_{i-1,j+1}^n) (v_{i-1,j}^{n+1} + v_{i,j}^{n+1}) - \frac{1}{Re} \frac{(v_{i,j}^{n+1} - v_{i-1,j}^{n+1})}{\Delta x}$$

$$F_{i,j+\frac{1}{2}}^2 = 0.25 (v_{i,j}^n + v_{i,j+1}^n) (v_{i,j}^{n+1} + v_{i,j+1}^{n+1}) - \frac{1}{Re} \frac{(v_{i,j+1}^{n+1} - v_{i,j}^{n+1})}{\Delta y}$$

$$F_{i,j-\frac{1}{2}}^2 = 0.25 (v_{i,j-1}^n + v_{i,j}^n) (v_{i,j-1}^{n+1} + v_{i,j}^{n+1}) - \frac{1}{Re} \frac{(v_{i,j}^{n+1} - v_{i,j-1}^{n+1})}{\Delta y}$$

Substituting E^2 and F^2 in Eq. (6.8) yields

$$\left(\frac{\Delta x \Delta y}{\Delta t} + a_{i,j}^v \right) v_{i,j}^{n+1} + \sum a_{nb}^v v_{nb}^{n+1} + b^v + \Delta x (p_{i,j+1}^{n+1} - p_{i,j}^{n+1}) = 0 \quad (6.9)$$

At any intermediate stage, the solution is to be advanced from n th time level to $(n+1)$ th time level. The term b^v equals $-\Delta x \Delta y v_{i,j}^n / \Delta t$. The velocity is advanced in two steps. First, the momentum equations (6.7) and (6.9) are solved to obtain the provisional values of u^* , and v^* . It is not possible to obtain u^{n+1} and v^{n+1} directly since the provisional velocities have not satisfied the continuity equation as yet.

Making use of the approximate velocity solution \mathbf{u}^* , a pressure correction δp will evolve which will give $p^{n+1} = p^n + \delta p$ and also a velocity correction \mathbf{u}^c will be obtainable. As such, \mathbf{u}^c will correct \mathbf{u}^* in such a manner that $\mathbf{u}^{n+1} = \mathbf{u}^* + \mathbf{u}^c$ and \mathbf{u}^{n+1} will satisfy the continuity Eq. (6.5).

In order to obtain \mathbf{u}^* , Eqns. (6.7) and (6.9) are approximated as

$$\left(\frac{\Delta x \Delta y}{\Delta t} + a_{i,j}^u \right) u_{i,j}^* + \sum a_{nb}^u u_{nb}^* = -b^u - \Delta y (p_{i+1,j}^n - p_{i,j}^n) \quad (6.10)$$

$$\left(\frac{\Delta x \Delta y}{\Delta t} + a_{i,j}^v \right) v_{i,j}^* + \sum a_{nb}^v v_{nb}^* = -b^v - \Delta x (p_{i,j+1}^n - p_{i,j}^n) \quad (6.11)$$

6.3.3 Solution Procedure

The Eqns. (6.10) and (6.11) can be evaluated in an implicit manner. For example, in Eq. (6.10) $u_{i,j}^*$ and all the neighbors, $u_{i+1,j}^*$, $u_{i-1,j}^*$, $u_{i,j+1}^*$, and $u_{i,j-1}^*$ are unknowns and they can be expressed as a system of equations by substitution of $i = 2$ to $(imax - 1)$ and $j = 2$ to $(jmax - 1)$. This will involve, solution of a penta-diagonal matrix. Patankar (1980) splits the evaluation procedure. At the first place, he writes Eqns. (6.10) and (6.11) as tridiagonal systems along each x -grid line (j constant) and solves them using Thomas algorithm. In a subsequent step, Eqns. (6.10) and (6.11) are written as tridiagonal systems along each y -grid line (i constant) and solves them using Thomas algorithm. This is equivalent to implicit evaluation using ADI scheme. Now, if we subtract Eq. (6.10) from Eq. (6.7), we shall obtain

$$\left(\frac{\Delta x \Delta y}{\Delta t} + a_{i,j}^u \right) u_{i,j}^c = \sum a_{nb}^u u_{nb}^c - \Delta y (\delta p_{i+1,j} - \delta p_{i,j}) \quad (6.12)$$

In a similar manner, Eq. (6.11) is subtracted from Eq. (6.9) to produce a correction equation for v^c .

$$\left(\frac{\Delta x \Delta y}{\Delta t} + a_{i,j}^v \right) v_{i,j}^c = \sum a_{nb}^v v_{nb}^c - \Delta x (\delta p_{i,j+1} - \delta p_{i,j}) \quad (6.13)$$

In order to make the link between u^c and δp explicit, Eq. (6.12) can be reduced to

$$u_{i,j}^c = \frac{E_1 \Delta y (\delta p_{i,j} - \delta p_{i+1,j})}{(1 + E_1) a_{i,j}^u} \quad (6.14)$$

where $E_1 = \Delta t a_{i,j}^u / \Delta x \Delta y$

An equivalent expression can be obtained for $v_{i,j}^c$ as

$$v_{i,j}^c = \frac{E_2 \Delta x (\delta p_{i,j} - \delta p_{i,j+1})}{(1 + E_2) a_{i,j}^v} \quad (6.15)$$

where $E_2 = \Delta t a_{i,j}^v / \Delta x \Delta y$

Now, substitution of $u_{i,j}^{n+1} = u_{i,j}^* + u_{i,j}^c$ and $v_{i,j}^{n+1} = v_{i,j}^* + v_{i,j}^c$ into (6.5) and use of (6.14) and (6.15) produces

$$a_{i,j}^p \delta p_{i,j} = \sum a_{nb}^p \delta p_{nb} + b^p \quad (6.16)$$

where, $b^p = -(u_{i,j}^* - u_{i-1,j}^*) \Delta y - (v_{i,j}^* - v_{i,j-1}^*) \Delta x$. Eq. (6.16) is basically a discrete form of Poisson equation that is equivalent to

$$\nabla^2(\delta p) = \frac{1}{\Delta t} \nabla \cdot \mathbf{u}^* \quad (6.17)$$

Eq. (6.14) and (6.15) can also be represented as

$$\mathbf{u}^c = -\frac{1}{\Delta t} \nabla(\delta p) \quad (6.18)$$

The algorithm may be summarized as

6.10 Computational Fluid Dynamics

1. \mathbf{u}^* is obtained from equations (6.10) and (6.11).
2. δp is obtained from equation (6.16).
3. \mathbf{u}^c is obtained from equations (6.14) and (6.15).
4. p^{new} is obtained from $p^{new} = p^n + \alpha \delta p$, where α is a relaxation parameter.
5. Calculate updated $u_{i,j}$, $v_{i,j}$ from their starred values using velocity correction formulae $u_{i,j}^{new} = u_{i,j}^* + u_{i,j}^c$ and $v_{i,j}^{new} = v_{i,j}^* + v_{i,j}^c$
6. Treat the corrected pressure p^{new} as new initial pressure p^n . Use $u_{i,j}^{new}$ and $v_{i,j}^{new}$ as $u_{i,j}^n$ and $v_{i,j}^n$. Calculate new \mathbf{u}^* from equations (6.10) and (6.11). Repeat (2-5), the entire procedure until a converged solution is obtained. It may be noted that the solution converges as $b^p = 0$.

Patankar (1980) introduced a revised algorithm, SIMPLER to improve the situation. The SIMPLER algorithm has the following steps.

1. A velocity field $\hat{\mathbf{u}}$ is computed from equations (6.10) and (6.11).
2. equation (6.16) then becomes a Poisson equation for p^{n+1} rather than δp with $\hat{\mathbf{u}}$ replacing the \mathbf{u}^* terms in b.
3. The p^{n+1} (obtained from step 2) replaces p^n in equations (6.10) and (6.11), which are solved for \mathbf{u}^* (as it was done in SIMPLE).
4. Equation (6.16) is solved for δp and it is used to provide $\mathbf{u}^{n+1} = \mathbf{u}^* + \mathbf{u}^c$ but no further adjustment is made to p^{n+1} .

Van Doormal and Raithby (1984) proposed SIMPLEC which is another modified version of SIMPLE algorithm and gives faster convergence.

6.3.4 Two-dimensional System of Equations and Line-by-line TDMA

Whether the discretized momentum Eqns. (6.10) and (6.11) or the pressure correction Eq. (6.16) the final outcome is a system of algebraic equation given by $a_P \phi_P = a_E \phi_E + a_W \phi_W + a_N \phi_N + a_S \phi_S + b$. The current values of the dependent variables (ϕ 's) are to be evaluated from the known values of the coefficients (a's). The evaluation algorithm will be same for the momentum equations and the pressure correction equation. On a rectangular grid, the dependent variables at one point (i, j) may be expressed in terms of its neighbors (Fig. 6.5) as

$$a_{i,j} u_{i,j} = b_{i,j} u_{i+1,j} + c_{i,j} u_{i-1,j} + d_{i,j} u_{i,j+1} + e_{i,j} u_{i,j-1} + f_{i,j}$$

where $b_{i,j}$ is equivalent to a_E , $c_{i,j}$ to a_W , $d_{i,j}$ to a_N , $e_{i,j}$ to a_S and $f_{i,j}$ to b . The evaluation of u can be accomplished in the following ways:

(a) Vertical Sweep Upwards may be written in a pseudo FORTRAN code as

```
DO 10 J = 2, M - 1
DO 10 I = 2, L - 1
```

$$10 \quad a_{i,j} u_{i,j} = b_{i,j} u_{i+1,j} + c_{i,j} u_{i-1,j} + (d_{i,j} \bar{u}_{i,j+1} + e_{i,j} \bar{u}_{i,j-1} + f_{i,j})$$

Here \bar{u} is the currently available value in storage and all the coefficients including $f_{i,j}$ are known. for each j , we shall get a system of equations if we substitute $i = 2, \dots, L - 1$. In other words, for each j , a tridiagonal matrix is available which can be solved for all i row of points at that j . Once one complete row is evaluated for any particular j , the next j will be taken up, and so on.

(b) Horizontal Sweep Forward may be written in pseudo FORTRAN code as

```
DO 20 I = 2, L - 1
DO 20 J = 2, M - 1
```

$$20 \quad a_{i,j} u_{i,j} = d_{i,j} u_{i,j+1} + e_{i,j} u_{i,j-1} + (b_{i,j} \bar{u}_{i+1,j} + c_{i,j} \bar{u}_{i-1,j} + f_{i,j})$$

Again \bar{u} is the currently available value in storage from previous calculations.

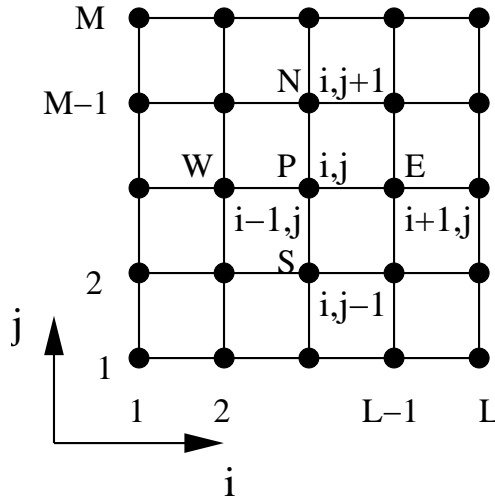


Figure 6.5: Dependent variable at (i, j) is expressed in terms of neighboring points.

For each i , we get a system of equation if we substitute $j = 2, \dots, M - 1$. A tridiagonal matrix is available for each i . Once one complete column of points

are evaluated for any particular i , the next i will be taken up and so on. The vertical sweep upward and downward are repeated. Similarly the horizontal sweep forward and rearward are also repeated until convergence is achieved. For solving tridiagonal system, the tridiagonal matrix algorithm (TDMA) due to Thomas (1949) is deployed. The above mentioned evaluation procedure is known as line-by-line TDMA.

6.4 Solution of the Unsteady Navier-Stokes Equations

6.4.1 Introduction to the MAC method

The MAC method of Harlow and Welch is one of the earliest and most useful methods for solving the Navier-Stokes equations. This method necessarily deals with a Poisson equation for the pressure and momentum equations for the computation of velocity. It was basically developed to solve problems with free surfaces, but can be applied to any incompressible fluid flow problem. A modified version of the original MAC method due to Hirt and Cook (1972) has been used by researchers to solve a variety of flow problems.

The text discusses the modified MAC method and highlights the salient features of the solution algorithm so that the reader is able to write a computer program with some confidence. The important ideas on which the MAC algorithm is based are:

1. Unsteady Navier-Stokes equations for incompressible flows in weak conservative form and the continuity equation are the governing equations.
2. Description of the problem is elliptic in space and parabolic in time. Solution will be marched in the time direction. At each time step, a converged solution in space is obtained but this converged solution at any time step may not be the solution of the physical problem.
3. If the problem is steady, in its physical sense, then after a finite number of steps in time direction, two consecutive time steps will show identical solutions. However, in a machine-computation this is not possible hence a very small upper bound, say, "STAT" is predefined. Typically, STAT may be chosen between 10^{-3} and 10^{-5} . If the maximum discrepancy of any of the velocity components for two consecutive time steps for any location over the entire space does not exceed STAT, then it can be said that the steady solution has been evolved.
4. If the physical problem is basically unsteady in nature, the aforesaid maximum discrepancy of any dependant variable for two consecutive time steps will never be less than STAT. However, for such a situation, a specified velocity component can be stored over a long duration of time and plot of

the velocity component against time (often called as signal) depicts the character of the flow. Such a flow may be labelled simply as “unsteady”.

5. With the help of the momentum equations, we compute explicitly a provisional value of the velocity components for the next time step.

Consider the weak conservative form of the nondimensional momentum equation in the x -direction:

$$\frac{\partial u}{\partial t} + \frac{\partial(u^2)}{\partial x} + \frac{\partial(uv)}{\partial y} + \frac{\partial(uw)}{\partial z} = -\frac{\partial p}{\partial x} + \frac{1}{Re} \nabla^2 u$$

It is assumed that at $t = n^{th}$ level, we have a converged solution. Then for the next time step

$$\frac{\tilde{u}_{i,j,k}^{n+1} - u_{i,j,k}^n}{\Delta t} = [CONDIFU - DPDX]_{i,j,k}^n$$

or

$$\tilde{u}_{i,j,k}^{n+1} = u_{i,j,k}^n + \Delta t [CONDIFU - DPDX]_{i,j,k}^n \quad (6.19)$$

$[CONDIFU - DPDX]_{i,j,k}^n$ consists of convective and diffusive terms, and the pressure gradient. Similarly, the provisional values for $\tilde{v}_{i,j,k}^{n+1}$ and $\tilde{w}_{i,j,k}^{n+1}$ can be explicitly computed. These explicitly advanced velocity components may not constitute a realistic flow field. A divergence-free velocity field has to exist in order to describe a plausible incompressible flow situation. Now, with these provisional $\tilde{u}_{i,j,k}^{n+1}$, $\tilde{v}_{i,j,k}^{n+1}$ and $\tilde{w}_{i,j,k}^{n+1}$ values, continuity equation is evaluated in each cell. If $(\nabla \cdot V)$ produces a nonzero value, there must be some amount of mass accumulation or annihilation in each cell which is not physically possible. Therefore the pressure at any cell is directly linked with the value of the $(\nabla \cdot V)$ of that cell. Now, on one hand the pressure has to be calculated with the help of the nonzero divergence value and on the other, the velocity components have to be adjusted. The correction procedure continues through an iterative cycle until the divergence-free velocity field is ensured. Details of the procedure will be discussed in the subsequent section.

6. Boundary conditions are to be applied after each explicit evaluation for the time step is accomplished. Since the governing equations are elliptic in space, boundary conditions on all confining surfaces are required. Moreover, the boundary conditions are also to be applied after every pressure-velocity iteration. The five types of boundary conditions to be considered are rigid no-slip walls, free-slip walls, inflow and outflow boundaries, and periodic (repeating) boundaries.

6.4.2 MAC Formulation

The region in which computations are to be performed is divided into a set of small cells having edge lengths δx , δy and δz (Fig. 6.6). With respect to this set of computational cells, velocity components are located at the centre of the cell faces to which they are normal and pressure and temperature are defined at the centre of the cells. Cells are labeled with an index (i, j, k) which denotes the cell number as counted from the origin in the x , y and z directions respectively. Also $p_{i,j,k}$ is the pressure at the centre of the cell (i, j, k) , while $u_{i,j,k}$ is the x -direction velocity at the centre of the face between cells (i, j, k) and $(i + 1, j, k)$ and so on (Fig. 6.7). Because of the staggered grid arrangements, the velocities are not defined at the nodal points, but whenever required, they are to be found by interpolation. For example, with uniform grids, we can write $u_{i-1/2,j,k} = \frac{1}{2}[u_{i-1,j,k} + u_{i,j,k}]$. Where a product or square of such a quantity appears, it is to be averaged first and then the product to be formed.

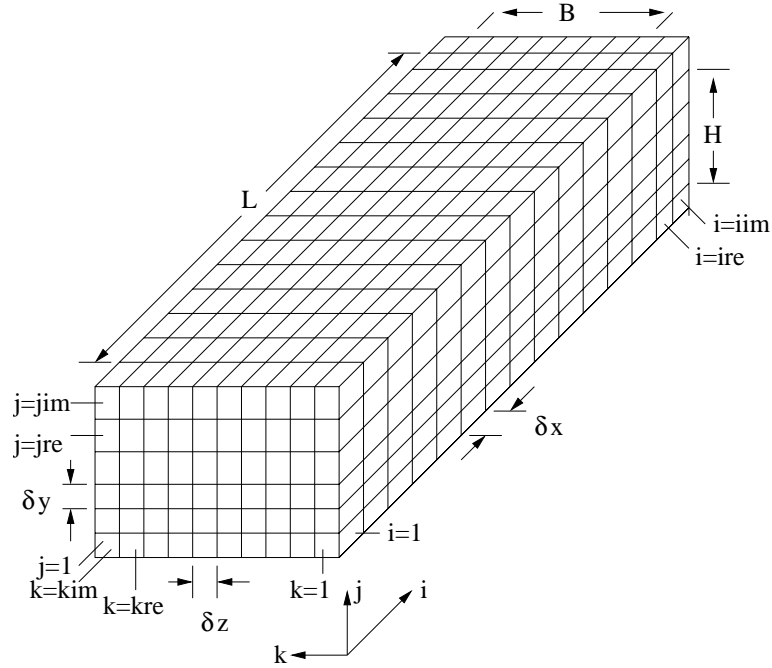


Figure 6.6: Discretization of a three-dimensional domain.

Convective terms are discretized using a weighted averaged of second upwind and space centered scheme (Hirt et al., 1975). Diffusive terms are discretized by a central differencing scheme. Let us consider the discretized terms of the x -momentum equation (Figure 6.7):

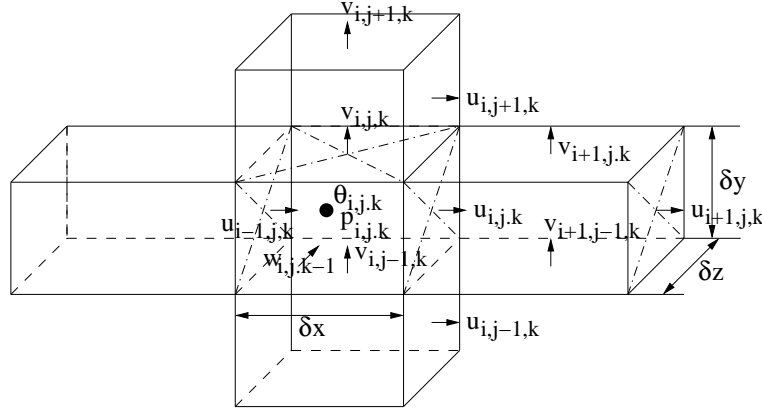


Figure 6.7: Three-dimensional staggered grid showing the locations of the discretized variables.

$$\begin{aligned}
 \frac{\partial(u^2)}{\partial x} &= \frac{1}{4\delta x} [(u_{i,j,k} + u_{i+1,j,k})(u_{i,j,k} + u_{i+1,j,k}) \\
 &\quad + \alpha |(u_{i,j,k} + u_{i+1,j,k})|(u_{i,j,k} - u_{i+1,j,k}) \\
 &\quad - (u_{i-1,j,k} + u_{i,j,k})(u_{i-1,j,k} + u_{i,j,k}) \\
 &\quad - \alpha |(u_{i-1,j,k} + u_{i,j,k})|(u_{i-1,j,k} - u_{i,j,k})] \\
 &\equiv DUUDX
 \end{aligned}$$

$$\begin{aligned}
 \frac{\partial(uv)}{\partial y} &= \frac{1}{4\delta y} [(v_{i,j,k} + v_{i+1,j,k})(u_{i,j,k} + u_{i,j+1,k}) \\
 &\quad + \alpha |(v_{i,j,k} + v_{i+1,j,k})|(u_{i,j,k} - u_{i,j+1,k}) \\
 &\quad - (v_{i,j-1,k} + v_{i+1,j-1,k})(u_{i,j-1,k} + u_{i,j,k}) \\
 &\quad - \alpha |(v_{i,j-1,k} + v_{i+1,j-1,k})|(u_{i,j-1,k} - u_{i,j,k})] \\
 &\equiv DUV DY
 \end{aligned}$$

$$\begin{aligned}
 \frac{\partial(uw)}{\partial z} &= \frac{1}{4\delta z} [(w_{i,j,k} + w_{i+1,j,k})(u_{i,j,k} + u_{i,j,k+1}) \\
 &\quad + \alpha |(w_{i,j,k} + w_{i+1,j,k})|(u_{i,j,k} - u_{i,j,k+1}) \\
 &\quad - (w_{i,j,k-1} + w_{i+1,j,k-1})(u_{i,j,k-1} + u_{i,j,k}) \\
 &\quad - \alpha |(w_{i,j,k-1} + w_{i+1,j,k-1})|(u_{i,j,k-1} - u_{i,j,k})] \\
 &\equiv DUWDZ
 \end{aligned}$$

$$\frac{\partial p}{\partial x} = \frac{p_{i+1,j,k} - p_{i,j,k}}{\delta x} \equiv DPDX$$

$$\frac{\partial^2 u}{\partial x^2} = \frac{u_{i+1,j,k} - 2u_{i,j,k} + u_{i-1,j,k}}{(\delta x)^2} \equiv D2UDX2$$

$$\frac{\partial^2 u}{\partial y^2} = \frac{u_{i,j+1,k} - 2u_{i,j,k} + u_{i,j-1,k}}{(\delta y)^2} \equiv D2UDY2$$

$$\frac{\partial^2 u}{\partial z^2} = \frac{u_{i,j,k+1} - 2u_{i,j,k} + u_{i,j,k-1}}{(\delta z)^2} \equiv D2UDZ2$$

with

$$\begin{aligned} \alpha &\longrightarrow 1 && \text{Scheme} \longrightarrow \text{Second Upwind} \\ \alpha &\longrightarrow 0 && \text{Scheme} \longrightarrow \text{Space centred} \end{aligned}$$

Factor α is chosen in such a way that the differencing scheme retains “something” of second-order accuracy and the required upwinding is done for the sake of stability. A typical value of α is between 0.2 and 0.3. As mentioned earlier, the quantity $\tilde{u}_{i,j,k}^{n+1}$ is now evaluated explicitly from the discretized form of Equation (6.2) as

$$\tilde{u}_{i,j,k}^{n+1} = u_{i,j,k}^n + \delta t [CONDIFU - DPDX]_{i,j,k}^n$$

where

$$\begin{aligned} [CONDIFU - DPDX]_{i,j,k}^n = & [(-DUUDX - DUV DY - DUW DZ) \\ & - DPDX + (1/Re)(D2UDX2 \\ & + D2UDY2 + D2UDZ2)] \end{aligned}$$

Similarly, we evaluate

$$\tilde{v}_{i,j,k}^{n+1} = v_{i,j,k}^n + \delta t [CONDIFV - DPDY]_{i,j,k}^n \quad (6.20)$$

$$\tilde{w}_{i,j,k}^{n+1} = w_{i,j,k}^n + \delta t [CONDIFW - DPDZ]_{i,j,k}^n \quad (6.21)$$

As discussed earlier, the explicitly advanced tilde velocities may not necessarily lead to a flow field with zero mass divergence in each cell. This implies that, at this stage the pressure distribution is not correct, the pressure in each cell will be corrected in such a way that there is no net mass flow in or out of the cell. In the original MAC method, the corrected pressures were obtained from the solution of a Poisson equation for pressure. A related technique developed by Chorin (1967) involved a simultaneous iteration on pressure and velocity components. Viece (1971) showed that the two methods as applied to MAC are equivalent. We shall make use of the iterative correction procedure of Chorin

(1967) in order to obtain a divergence-free velocity field. The mathematical methodology of this iterative pressure-velocity correction procedure will be discussed herein.

The relationship between the explicitly advanced velocity component and velocity at the previous time step may be written as

$$\tilde{u}_{i,j,k}^{n+1} = u_{i,j,k}^n + \delta t \frac{[p_{i,j,k}^n - p_{i+1,j,k}^n]}{\Delta x} + \delta t [CONDIFU]_{i,j,k}^n \quad (6.22)$$

where $[CONDIFU]_{i,j,k}^n$ is only the contribution from convection and diffusion terms. On the other hand, the corrected velocity component (unknown) will be related to the corrected pressure (also unknown) in the following way:

$$u_{i,j,k}^{n+1} = u_{i,j,k}^n + \delta t \frac{[p_{i,j,k}^{n+1} - p_{i+1,j,k}^{n+1}]}{\Delta x} + \delta t [CONDIFU]_{i,j,k}^n \quad (6.23)$$

From Equations (6.22) and (6.23)

$$u_{i,j,k}^{n+1} - \tilde{u}_{i,j,k}^{n+1} = \delta t \frac{[p'_{i,j,k} - p'_{i+1,j,k}]}{\delta x}$$

where the pressure correction may be defined as

$$p'_{i,j,k} = p_{i,j,k}^{n+1} - p_{i,j,k}^n$$

Neither the pressure correction nor is the quantity $u_{i,j,k}^{n+1}$ explicitly known at this stage. Hence, one cannot be calculated without the help of the other. Calculations are done in an iterative cycle and we write

corrected	Estimated	Correction
$u_{i,j,k}^{n+1}$	\longrightarrow	$\tilde{u}_{i,j,k}^{n+1} + \delta t \frac{[p'_{i,j,k} - p'_{i+1,j,k}]}{\delta x}$

In a similar way, we can formulate the following array:

$$u_{i,j,k}^{n+1} \longrightarrow \tilde{u}_{i,j,k}^{n+1} + \delta t \frac{[p'_{i,j,k} - p'_{i+1,j,k}]}{\delta x} \quad (6.24)$$

$$u_{i-1,j,k}^{n+1} \longrightarrow \tilde{u}_{i-1,j,k}^{n+1} - \delta t \frac{[p'_{i,j,k} - p'_{i-1,j,k}]}{\delta x} \quad (6.25)$$

$$v_{i,j,k}^{n+1} \longrightarrow \tilde{v}_{i,j,k}^{n+1} + \delta t \frac{[p'_{i,j,k} - p'_{i,j+1,k}]}{\delta y} \quad (6.26)$$

$$v_{i,j-1,k}^{n+1} \longrightarrow \tilde{v}_{i,j-1,k}^{n+1} - \delta t \frac{[p'_{i,j,k} - p'_{i,j-1,k}]}{\delta y} \quad (6.27)$$

$$w_{i,j,k}^{n+1} \longrightarrow \tilde{w}_{i,j,k}^{n+1} + \delta t \frac{[p'_{i,j,k} - p'_{i,j,k+1}]}{\delta z} \quad (6.28)$$

$$w_{i,j,k-1}^{n+1} \longrightarrow \tilde{w}_{i,j,k-1}^{n+1} - \delta t \frac{[p'_{i,j,k} - p'_{i,j,k-1}]}{\delta z} \quad (6.29)$$

The correction is done through the continuity equation. Plugging-in the above relationship into the continuity equation (6.1) yields

$$\begin{aligned}
& \left[\frac{u_{i,j,k}^{n+1} - u_{i-1,j,k}^{n+1}}{\delta x} + \frac{v_{i,j,k}^{n+1} - v_{i,j-1,k}^{n+1}}{\delta y} + \frac{w_{i,j,k}^{n+1} - w_{i,j,k-1}^{n+1}}{\delta z} \right] \\
&= \left[\frac{\tilde{u}_{i,j,k}^{n+1} - \tilde{u}_{i-1,j,k}^{n+1}}{\delta x} + \frac{\tilde{v}_{i,j,k}^{n+1} - \tilde{v}_{i,j-1,k}^{n+1}}{\delta y} + \frac{\tilde{w}_{i,j,k}^{n+1} - \tilde{w}_{i,j,k-1}^{n+1}}{\delta z} \right] \\
&- \delta t \left[\frac{p'_{i+1,j,k} - 2p'_{i,j,k} + p'_{i-1,j,k}}{(\delta x)^2} + \frac{p'_{i,j+1,k} - 2p'_{i,j,k} + p'_{i,j-1,k}}{(\delta y)^2} \right. \\
&\quad \left. + \frac{p'_{i,j,k+1} - 2p'_{i,j,k} + p'_{i,j,k-1}}{(\delta z)^2} \right] \tag{6.30}
\end{aligned}$$

or

$$\begin{aligned}
& \left[\frac{u_{i,j,k}^{n+1} - u_{i-1,j,k}^{n+1}}{\delta x} + \frac{v_{i,j,k}^{n+1} - v_{i,j-1,k}^{n+1}}{\delta y} + \frac{w_{i,j,k}^{n+1} - w_{i,j,k-1}^{n+1}}{\delta z} \right] \\
&= \left[\frac{\tilde{u}_{i,j,k}^{n+1} - \tilde{u}_{i-1,j,k}^{n+1}}{\delta x} + \frac{\tilde{v}_{i,j,k}^{n+1} - \tilde{v}_{i,j-1,k}^{n+1}}{\delta y} + \frac{\tilde{w}_{i,j,k}^{n+1} - \tilde{w}_{i,j,k-1}^{n+1}}{\delta z} \right] \\
&\quad + \frac{2 \delta t (p'_{i,j,k})}{\delta x^2} + \frac{2 \delta t (p'_{i,j,k})}{\delta y^2} + \frac{2 \delta t (p'_{i,j,k})}{\delta z^2} \tag{6.31}
\end{aligned}$$

In deriving the above expression, it is assumed that the pressure corrections in the neighboring cells are zero. Back to the calculations, we can write

$$0 = (Div)_{i,j,k} + p'_{i,j,k} \left[2\delta t \left(\frac{1}{\delta x^2} + \frac{1}{\delta y^2} + \frac{1}{\delta z^2} \right) \right]$$

or

$$p'_{i,j,k} = \frac{-(Div)_{i,j,k}}{\left[2\delta t \left(\frac{1}{\delta x^2} + \frac{1}{\delta y^2} + \frac{1}{\delta z^2} \right) \right]} \tag{6.32}$$

In order to accelerate the calculation, the pressure correction equation is modified as

$$p'_{i,j,k} = \frac{-\omega_0 (Div)_{i,j,k}}{\left[2\delta t \left(\frac{1}{\delta x^2} + \frac{1}{\delta y^2} + \frac{1}{\delta z^2} \right) \right]} \tag{6.33}$$

where ω_0 is the overrelaxation factor. A value of $\omega_0 = 1.7$ is commonly used. The value of ω_0 giving most rapid convergence, should be determined by numerical experimentation. After calculating $p'_{i,j,k}$, the pressure in the cell (i, j, k) is adjusted as

$$p_{i,j,k}^{n+1} \longrightarrow p_{i,j,k}^n + p'_{i,j,k} \tag{6.34}$$

Now the pressure and velocity components for each cell are corrected through an iterative procedure in such a way that for the final pressure field, the velocity divergence in each cell vanishes. The process is continued till a divergence-free velocity is reached with a prescribed upper bound; here a value of 0.0001 is recommended.

Finally, we discuss another important observation. If the velocity boundary conditions are correct and a divergence-free converged velocity field has been obtained, eventually correct pressure will be determined in all the cells at the boundary. Thus, this method avoids the application of pressure boundary conditions. This typical feature of modified MAC method has been discussed in more detail by Peyret and Taylor (1983). However, it was also shown by Brandt, Dendy and Ruppel (1980) that the aforesaid pressure-velocity iteration procedure of correcting pressure is equivalent to the solution of Poisson equation for pressure. As such from Eqn. (6.30) we can directly write as

$$\nabla^2(p'_{i,j,k}) = \frac{(Div)_{i,j,k}}{\delta t} \quad (6.35)$$

The Eqn. (6.35) can be solved implicitly using appropriate boundary conditions for p' at the confining boundaries.

6.4.3 Boundary Conditions

So far we have not discussed the boundary conditions. However, they are imposed by setting appropriate velocities in the fictitious cells surrounding the physical domain (Figure 6.8).

Consider, for example, the bottom boundary of the computational (physical) mesh. If this boundary is to be a rigid no-slip wall, the normal velocity on the wall must be zero and the tangential velocity components should also be zero. Here we consider a stationary wall. With reference to the Figure 6.8, we have

$$\left. \begin{aligned} v_{i,1,k} &= 0 \\ u_{i,1,k} &= -u_{i,2,k} \\ w_{i,1,k} &= -w_{i,2,k} \end{aligned} \right\} \begin{array}{l} \text{for } i = 2 \text{ to } ire \\ \text{and } k = 2 \text{ to } kre \end{array}$$

If the right side of the wall is a free-slip (vanishing shear) boundary, the normal velocity must be zero and the tangential velocities should have no normal gradient.

$$\left. \begin{aligned} w_{i,j,1} &= 0 \\ u_{i,j,1} &= u_{i,j,2} \\ v_{i,j,1} &= v_{i,j,2} \end{aligned} \right\} \begin{array}{l} \text{for } i = 2 \text{ to } ire \\ \text{and } j = 2 \text{ to } jre \end{array}$$

If the front plane is provided with inflow boundary conditions, it should be specified properly. Any desired functional relationship may be recommended. Generally, normal velocity components are set to zero and a uniform or parabolic

axial velocity may be deployed. Hence with reference to Fig. 6.8, we can write

$$\left. \begin{aligned} v_{1,j,k} &= -v_{2,j,k} \\ w_{1,j,k} &= -w_{2,j,k} \\ u_{1,j,k} &= 1.0 \quad \text{or} \\ u_{1,j,k} &= 1.5 \left[1 - ((j_m - j)/j_m)^2 \right] \end{aligned} \right\} \begin{array}{l} \text{for } j = 2 \text{ to } j_{re} \\ \text{and } k = 2 \text{ to } k_{re} \end{array}$$

where j_m is the horizontal midplane.

Continuative or outflow boundaries always pose a problem for low-speed

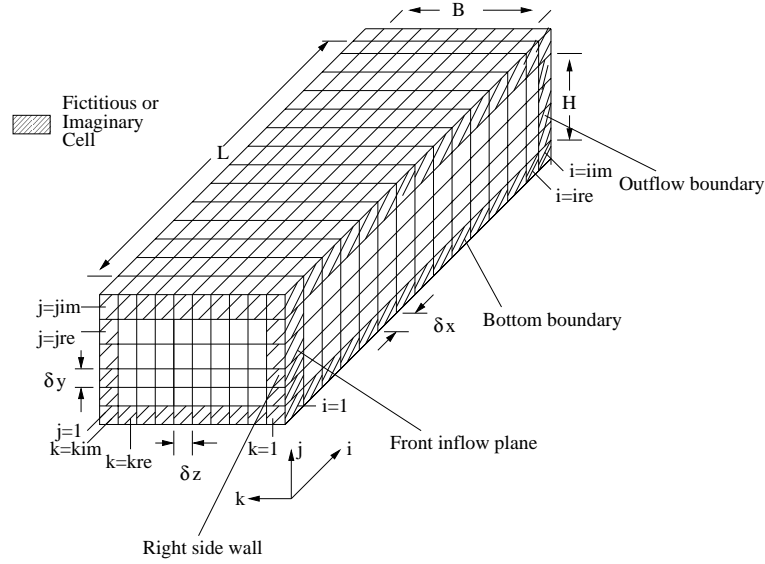


Figure 6.8: Boundary conditions and fictitious boundary cells.

calculations, because whatever prescription is chosen it can affect the entire flow upstream. What is needed is a prescription that permits fluid to flow out of the mesh with a minimum of upstream influence. Commonly used conditions for such a boundary is $\nabla \mathbf{V} \cdot \mathbf{n} = 0$, where \mathbf{n} is the unit normal vector.

The boundary condition that has more generality at the outflow is described by Orlanski (1971). This condition allows changes inside the flow field to be transmitted outward, but not vice-versa:

$$\frac{\partial \Psi}{\partial t} + U_{av} \frac{\partial \Psi}{\partial x} = 0$$

where U_{av} is the average velocity at the outflow plane and Ψ represents u , v , w or any dependent variable.

6.4.4 Numerical Stability Considerations

For accuracy, the mesh size must be chosen small enough to resolve the expected spatial variations in all dependent variables. Once a mesh has been chosen, the choice of the time increment is governed by two restrictions, namely, the Courant-Fredrichs-Lewy (CFL) condition and the restriction on the basis of grid-Fourier numbers. According to the CFL condition, material cannot move through more than one cell in one time step, because the difference equations assume fluxes only between the adjacent cells. Therefore, the time increment must satisfy the inequality.

$$\delta t < \min \left\{ \frac{\delta x}{|u|}, \frac{\delta y}{|v|}, \frac{\delta z}{|w|} \right\} \quad (6.36)$$

where the minimum is with respect to every cell in the mesh. Typically, δt is chosen equal to one-fourth to one-third of the minimum cell transit time. When the viscous diffusion terms are more important, the condition necessary to ensure stability is dictated by the restriction on the Grid-Fourier numbers, which results in

$$\nu \delta t < \frac{1}{2} \cdot \frac{(\delta x^2 \delta y^2 \delta z^2)}{(\delta x^2 + \delta y^2 + \delta z^2)} \quad (6.37)$$

in dimensional form. After non-dimensionalization, this leads to

$$\delta t < \frac{1}{2} \cdot \frac{(\delta x^2 \delta y^2 \delta z^2)}{(\delta x^2 + \delta y^2 + \delta z^2)} Re \quad (6.38)$$

The final δt for each time increment is the minimum of the δt 's obtained from Equations (6.36) and (6.38)

The last quantity needed to ensure numerical stability is the upwind parameter α . In general, α should be slightly larger than the maximum value of $|u\delta t/\delta x|$ or $|v\delta t/\delta y|$ occurring in the mesh, that is,

$$\max \left\{ \left| \frac{u\delta t}{\delta x} \right|, \left| \frac{v\delta t}{\delta y} \right|, \left| \frac{w\delta t}{\delta z} \right| \right\} \leq \alpha < 1 \quad (6.39)$$

As a ready prescription, a value between 0.2 and 0.4 can be used for α . If α is too large, an unnecessary amount of numerical diffusion (artificial viscosity) will be introduced.

6.4.5 Higher-Order Upwind Differencing

More accurate solutions are obtained if the convective terms are discretized by higher-order schemes. Davis and Moore (1982) use the MAC method with a multidimensional third-order upwinding scheme. Needless to mention that their marching algorithm for the momentum equation is explicit and the stability restriction concerning the CFL condition [$u\delta t/\delta x \leq 1$ and $v\delta t/\delta y \leq 1$] is satisfied.

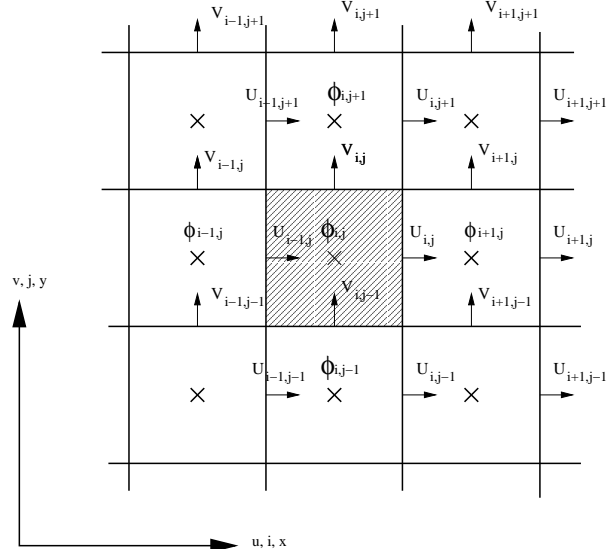


Figure 6.9: Dependent variables(u , v and ϕ) on a rectangular grid.

The multidimensional third-order upwinding is in principle similar to one dimensional quadratic upstream interpolation scheme introduced by Leonard (1979). Consider Fig. 6.9. Let ϕ be any property which can be convected and diffused. The convective term $\frac{\partial(u\phi)}{\partial x}$ may be represented as

$$\frac{\partial(u\phi)}{\partial x} = \frac{(u\phi)_{i+\frac{1}{2},j} - (u\phi)_{i-\frac{1}{2},j}}{\delta x} \quad (6.40)$$

where the variables $\phi_{i+\frac{1}{2},j}$ and $\phi_{i-\frac{1}{2},j}$ are defined as

$$\phi_{i+\frac{1}{2},j} = 0.5(\phi_{i,j} + \phi_{i+1,j}) - \frac{\xi}{3}(\phi_{i-1,j} - 2\phi_{i,j} + \phi_{i+1,j}) \quad \text{for } u_{i,j} \leq 0 \quad (6.41)$$

and

$$\phi_{i-\frac{1}{2},j} = 0.5(\phi_{i,j} + \phi_{i-1,j}) - \frac{\xi}{3}(\phi_{i-2,j} - 2\phi_{i-1,j} + \phi_{i,j}) \quad \text{for } u_{i,j} > 0 \quad (6.42)$$

The parameter ξ can be chosen to increase the accuracy or to alter the diffusion-like characteristics. It may be pointed out $\xi = 3/8$ corresponds to the QUICK scheme of Leonard(1979).

Let us consider two-dimensional momentum equation in weak conservative form which is given by

$$\frac{\partial u}{\partial t} + \frac{\partial(u^2)}{\partial x} + \frac{\partial(uv)}{\partial y} = -\frac{\partial p}{\partial x} + \frac{1}{Re} \left[\frac{\partial^2 u}{\partial x^2} + \frac{\partial^2 u}{\partial y^2} \right] \quad (6.43)$$

In non-conservative form this may be written as

$$\frac{\partial u}{\partial t} + u \frac{\partial u}{\partial x} + v \frac{\partial u}{\partial y} = -\frac{\partial p}{\partial x} + \frac{1}{Re} \left[\frac{\partial^2 u}{\partial x^2} + \frac{\partial^2 u}{\partial y^2} \right] \quad (6.44)$$

Here we introduce a term transport-velocity. The transport velocities for the second and third terms on the left hand side are u and v respectively. While dealing with the equations in the conservative form, we shall keep this in mind. For example, during discretization of the term $\partial(uv)/\partial y$ of Eq. (6.43) we should remember that v is the transport-velocity associated with this term. It is customary to define the transport-velocity at the nodal point where the equation is being defined. In case of the term $\partial(uv)/\partial y$ we have to refer to Fig. 6.10 and write down the product term uv as

$$(uv)_{i,j} = 0.25u_{i,j}(v_{i,j} + v_{i+1,j} + v_{i,j-1} + v_{i+1,j-1}) \quad (6.45)$$

Finally the discretization of the term $\partial(uv)/\partial y$ for the x -momentum equation will be accomplished in the following way:

$$\begin{aligned} \frac{\partial(uv)}{\partial y} = & 0.25 \frac{1}{8\delta y} \\ & [3u_{i,j+1}(v_{i,j+1} + v_{i,j} + v_{i+1,j+1} + v_{i+1,j}) \\ & + 3u_{i,j}(v_{i,j} + v_{i,j-1} + v_{i+1,j} + v_{i+1,j-1}) \\ & - 7u_{i,j-1}(v_{i,j-1} + v_{i,j-2} + v_{i+1,j-1} + v_{i+1,j-2}) \\ & + u_{i,j-2}(v_{i,j-2} + v_{i,j-3} + v_{i+1,j-2} + v_{i+1,j-3})] \quad \text{for } V > 0 \end{aligned} \quad (6.46)$$

$$\begin{aligned} \frac{\partial(uv)}{\partial y} = & 0.25 \frac{1}{8\delta y} \\ & [-u_{i,j+2}(v_{i,j+2} + v_{i,j+1} + v_{i+1,j+2} + v_{i+1,j+1}) \\ & + 7u_{i,j+1}(v_{i,j+1} + v_{i,j} + v_{i+1,j+1} + v_{i+1,j}) \\ & - 3u_{i,j}(v_{i,j} + v_{i,j-1} + v_{i+1,j} + v_{i+1,j-1}) \\ & - 3u_{i,j-1}(v_{i,j-1} + v_{i,j-2} + v_{i+1,j-1} + v_{i+1,j-2})] \quad \text{for } V < 0 \end{aligned} \quad (6.47)$$

where

$$V = v_{i,j} + v_{i+1,j} + v_{i,j-1} + v_{i+1,j-1}$$

6.4.6 Sample Results

For unsteady laminar flow past a rectangular obstacle in a channel, Mukhopadhyay, Biswas and Sundararajan (1992) use the MAC algorithm to explicitly march in time. Their results corroborated with the experimental observation of Okajima (1982). A typical example of numerical flow visualization depicting the development of von Kármán vortex street is illustrated in Fig. 6.11. The cross-stream vorticity contours vectors behind a delta-winglet placed inside a

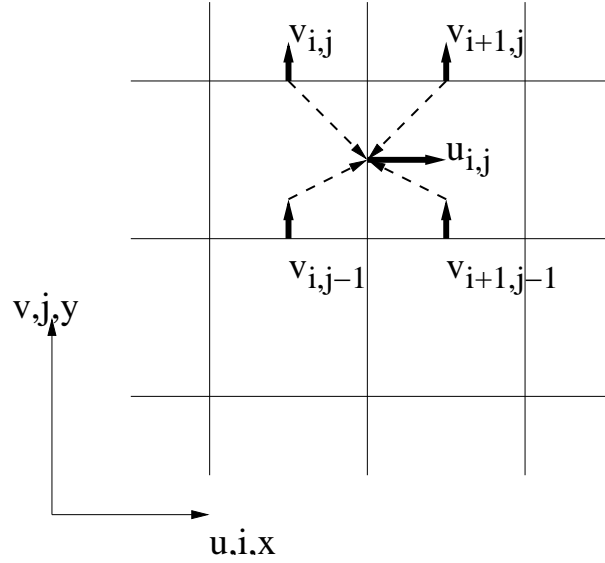


Figure 6.10: Definition of the transport velocity at a point where the momentum equation is being discretized.

channel are shown in Fig. 6.12. These results were obtained by Biswas, Torii et al. (1996) who used MAC to solve for a three-dimensional flow field in a channel containing delta-winglet as a vortex generator. The MAC algorithm has been extensively used by the researchers to solve flows in complex geometry. Braza, Chassaing and Ha-Minh (1986) investigated the dynamic characteristics of the pressure and velocity fields of the unsteady wake behind a circular cylinder using MAC algorithm. Robichaux, Tafti and Vanka (1992) deployed MAC algorithm for Large Eddy Simulation (LES) of turbulent channel flows. Of course, they performed the time integration of the discretized equations by using a fractional step method (Kim and Moin, 1985). Another investigation by Kim and Benson (1992) suggests that the MAC method is significantly accurate and at the same time the computational effort is reasonable.

6.5 Solution of Energy Equation

The energy equation for incompressible flows, neglecting mechanical work and gas radiation, may be written as

$$\rho c_p \left[\frac{\partial T}{\partial t^*} + u^* \frac{\partial T}{\partial x^*} + v^* \frac{\partial T}{\partial y^*} + w^* \frac{\partial T}{\partial z^*} \right] = k \nabla^2 T + \mu \phi^* \quad (6.48)$$



Figure 6.11: Streamlines crossing the cylinder in the duct: $Re_B = 162$

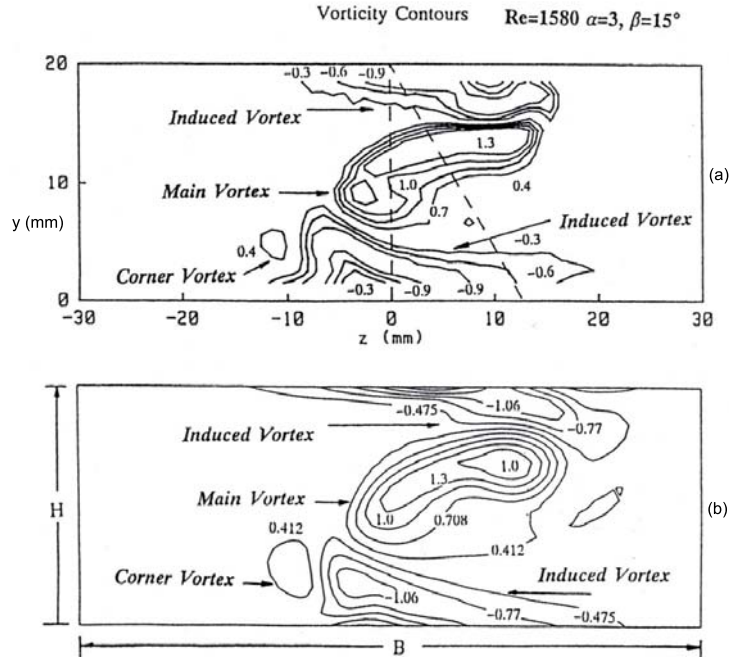


Figure 6.12: (a) & (b) Vorticity contours behind a cross-plane $X_c = 2.5$ behind the winglet at $\beta = 15^\circ$ (a) experiment, (b) computation

where ϕ^* is the viscous dissipation given as

$$\begin{aligned} \phi^* = 2 & \left[\left(\frac{\partial u^*}{\partial x^*} \right)^2 + \left(\frac{\partial v^*}{\partial y^*} \right)^2 + \left(\frac{\partial w^*}{\partial z^*} \right)^2 \right] + \left\{ \frac{\partial u^*}{\partial x^*} + \frac{\partial v^*}{\partial y^*} \right\}^2 \\ & + \left\{ \frac{\partial w^*}{\partial y^*} + \frac{\partial v^*}{\partial z^*} \right\}^2 + \left\{ \frac{\partial w^*}{\partial x^*} + \frac{\partial u^*}{\partial z^*} \right\}^2 \end{aligned}$$

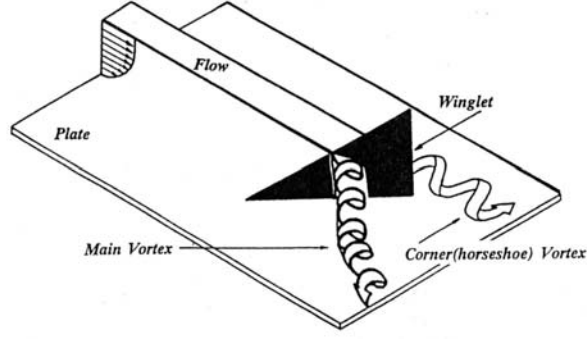


Figure 6.12(c) Formation of complex vortex system due to the winglet

Equation (6.48) may be non-dimensionalized in the following way:

$$u = \frac{u^*}{U_\infty}, \quad v = \frac{v^*}{U_\infty}, \quad w = \frac{w^*}{U_\infty}, \quad \theta = \frac{T - T_\infty}{T_w - T_\infty}$$

$$x = \frac{x^*}{L}, \quad y = \frac{y^*}{L}, \quad z = \frac{z^*}{L}, \quad t = \frac{t^*}{L/U_\infty}$$

Substituting the above variables in equation (6.48) we obtain

$$\begin{aligned} & \frac{\rho c_p U_\infty (T_w - T_\infty)}{L} \left[\frac{\partial \theta}{\partial t} + u \frac{\partial \theta}{\partial x} + v \frac{\partial \theta}{\partial y} + w \frac{\partial \theta}{\partial z} \right] \\ &= \frac{(T_w - T_\infty)k}{L^2} \left[\frac{\partial^2 \theta}{\partial x^2} + \frac{\partial^2 \theta}{\partial y^2} + \frac{\partial^2 \theta}{\partial z^2} \right] + \frac{\mu U_\infty^2}{L^2} \phi \end{aligned} \quad (6.49)$$

where ϕ is the nondimensional form of ϕ^* . Finally, the normalized energy equation becomes

$$\frac{\partial \theta}{\partial t} + u \frac{\partial \theta}{\partial x} + v \frac{\partial \theta}{\partial y} + w \frac{\partial \theta}{\partial z} = \frac{1}{Pe} \left[\frac{\partial^2 \theta}{\partial x^2} + \frac{\partial^2 \theta}{\partial y^2} + \frac{\partial^2 \theta}{\partial z^2} \right] + \frac{Ec}{Re} \phi \quad (6.50)$$

where Pe , the Peclet number is given as

$$\begin{aligned} \frac{1}{Pe} &= \frac{(T_w - T_\infty)k}{L^2} \cdot \frac{L}{\rho c_p U_\infty (T_w - T_\infty)} \\ \text{or } \frac{1}{Pe} &= \frac{k}{L \rho c_p U_\infty} = \frac{k}{\mu c_p} \cdot \frac{\mu}{\rho L U_\infty} = \frac{1}{Pr} \cdot \frac{1}{Re} \end{aligned}$$

Further, Ec , the Eckert number is

$$\frac{Ec}{Re} = \frac{\mu U_\infty^2}{L^2} \cdot \frac{L}{\rho c_p U_\infty (T_w - T_\infty)} = \frac{U_\infty^2}{c_p (T_w - T_\infty)} \cdot \frac{1}{\rho U_\infty L / \mu}$$

6.5.1 Retention of Dissipation

The dissipation term ϕ is frequently neglected while solving the energy equation for incompressible flows. As the Mach number $M \rightarrow 0$, $Ec \rightarrow 0$. However, even at a low Mach number, ϕ can be important if $(T_w - T_\infty)$ is very small. Let us look at these aspects. Since

$$Ec = \frac{U_\infty^2}{c_p(T_w - T_\infty)}, \quad \frac{1}{Ec} = \frac{c_p T_\infty}{U_\infty^2} \left[\frac{T_w}{T_\infty} - 1 \right]$$

and

$$\frac{c_p T_\infty}{U_\infty^2} = \frac{c_p \gamma R T_\infty}{\gamma R U_\infty^2}$$

where R is the gas constant $= c_p - c_v$, and $\gamma = c_p/c_v$.

Let the local acoustic velocity $C = \sqrt{\gamma R T_\infty}$, and Mach number $M_\infty = U_\infty/C$. Then,

$$\frac{c_p T_\infty}{U_\infty^2} = \frac{c_p}{\gamma(c_p - c_v)} \left[\frac{1}{M_\infty^2} \right] = \frac{c_p}{\gamma c_p \left(1 - \frac{1}{\gamma}\right)} \left[\frac{1}{M_\infty^2} \right] = \frac{1}{(\gamma - 1)} \frac{1}{M_\infty^2}$$

Hence,

$$\frac{1}{Ec} = \frac{1}{(\gamma - 1) M_\infty^2} \left(\frac{T_w}{T_\infty} - 1 \right)$$

or

$$Ec = \frac{(\gamma - 1) M_\infty^2}{\left(\frac{T_w}{T_\infty} - 1 \right)}$$

In general for incompressible flows $M_\infty < 0.3$ and $\gamma \geq 1$. Hence Ec is small. But for very small temperature difference, i.e., if T_w/T_∞ is slightly larger than 1, Ec might assume a large value and importance of dissipation arises.

However, for computing incompressible convective flows, the viscous dissipation is neglected in this chapter and we continue with the steady state energy equation.

6.6 Solution Procedure

The steady state energy equation, neglecting the dissipation term, may be written in the following conservative form as

$$\frac{\partial(u\theta)}{\partial x} + \frac{\partial(v\theta)}{\partial y} + \frac{\partial(w\theta)}{\partial z} = \frac{1}{Pe} \left[\frac{\partial^2 \theta}{\partial x^2} + \frac{\partial^2 \theta}{\partial y^2} + \frac{\partial^2 \theta}{\partial z^2} \right] \quad (6.51)$$

Equation (6.51) may be written as

$$\nabla^2 \theta = Pe [CONVT]_{i,j,k}^m \quad (6.52)$$

where $[CONVT]_{i,j,k}^m$ is the discretized convective terms on the left-hand side of Equation (6.51) and m stands for the iterative counter. To start with, we can assume any guess value of θ throughout the flow field. Since u , v , w are known from the solution of momentum equation hence Equation 6.51 is now a linear equation. However, from the guess value of θ and known correct values of u , v and w the left-hand side of Equation 6.51 is evaluated. A weighted average scheme or QUICK scheme may be adapted for discretization of the convective terms. After discretizing and evaluating right-hand side of Equation (6.52) we obtain a Poisson equation for the temperature with a source term on the right hand side. Now, we shall follow SOR technique for solving Equation (6.52). Consider a discretized equation as

$$\begin{aligned} \frac{\theta_{i+1,j,k} - 2\theta_{i,j,k} + \theta_{i-1,j,k}}{(\delta x)^2} + \frac{\theta_{i,j+1,k} - 2\theta_{i,j,k} + \theta_{i,j-1,k}}{(\delta y)^2} \\ + \frac{\theta_{i,j,k+1} - 2\theta_{i,j,k} + \theta_{i,j,k-1}}{(\delta z)^2} = S^{*m} \end{aligned}$$

where

$$S^{*m} \equiv Pe [CONVT]_{i,j,k}^m$$

or

$$A^{*m} - \theta_{i,j,k} \left[\left(\frac{2}{\delta x^2} + \frac{2}{\delta y^2} + \frac{2}{\delta z^2} \right) \right] = S^{*m}$$

or

$$\theta_{i,j,k} = \frac{A^{*m} - S^{*m}}{\left[\left(\frac{2}{\delta x^2} + \frac{2}{\delta y^2} + \frac{2}{\delta z^2} \right) \right]} \quad (6.53)$$

where

$$A^{*m} = \frac{\theta_{i+1,j,k}^m + \theta_{i-1,j,k}^m}{(\delta x)^2} + \frac{\theta_{i,j+1,k}^m + \theta_{i,j-1,k}^m}{(\delta y)^2} + \frac{\theta_{i,j,k+1}^m + \theta_{i,j,k-1}^m}{(\delta z)^2}$$

$\theta_{i,j,k}$ in Equation (6.53) may be assumed to be the most recent value and it may be written as $\theta_{i,j,k}^{m'}$. In order to accelerate the speed of computation we introduce an overrelaxation factor ω . Thus

$$\theta_{i,j,k}^{m+1} = \theta_{i,j,k}^m + \omega \left[\theta_{i,j,k}^{m'} - \theta_{i,j,k}^m \right] \quad (6.54)$$

where $\theta_{i,j,k}^m$ is the previous value, $\theta_{i,j,k}^{m'}$ the most recent value and $\theta_{i,j,k}^{m+1}$ the calculated better guess. The procedure will continue till the required convergence is achieved. This is equivalent to Gauss-Seidel procedure for solving a system of linear equations.

References

1. Biswas, G., Torii, K., Fujii, D., and Nishino, K., Numerical and Experimental Determination of Flow Structure and Heat Transfer Effects of Longitudinal Vortices in a Channel Flow, *Int. J. Heat Mass Transfer*, Vol. 39, pp. 3441-3451, 1996.
2. Biswas, G., Breuer, M. and Durst, M., Backward-Facing Step Flows for Various Expansion Ratios at Low and Moderate Reynolds Numbers, *Journal of Fluids Engineering (ASME)*, Vol. 126, pp. 362-374, 2004.
3. Brandt, A., Dendy, J.E and Ruppel, H., The Multigrid Method for Semi-Implicit Hydrodynamics Codes, *J. Comput. Phys*, Vol. 34, pp. 348-370, 1980.
4. Braza, M., Chassaing P. and Ha Minh, H., Numerical Study and Physical Analysis of the Pressure and Velocity Fields in the Near-Wake of a Circular Cylinder, *J. Fluid Mech.*, Vol. 165, pp. 79-130, 1986.
5. Chorin, A.J., Numerical Method for Solving Incompressible Viscous Flow Problems, *J. Comput. Phys.*, Vol. 2, pp. 12-26, 1967.
6. Davis, R.W. and Moore, E. F., A Numerical Study of Vortex Shedding from Rectangles, *J. Fluid Mech.*, 116: 475-506, 1982.
7. Harlow, F.H. and Welch, J.E., Numerical Calculation of Three-dependent Viscous Incompressible Flow of Fluid with Free Surfaces, *Phys. of Fluids*, Vol. 8, pp. 2182-2188, 1965.
8. Hirt, C.W. and Cook, J.L., Calculating Three-Dimensional Flows Around Structures and Over Rough Terrain, *J. Comput. Phys.*, Vol. 10, pp. 324-340, 1972.
9. Hirt, C.W., Nicholas, B.D. and Romera, N.C., Numerical Solution Algorithm for Transient Fluid Flows, LA-5852, *Los Alamos Scientific Laboratory Report*, 1975.
10. Kim, J. and Moin, P., Application of Fractional Step Method to Incompressible Navier-Stokes Equation, *J. Comput. Phys.*, Vol. 59, pp. 308-323, 1985.
11. Kim, S.W. and Benson, T.J., Comparison of the SMAC, PISO and Iterative Time Advancing Schemes for Unsteady Flows, *Computers & Fluids*, Vol. 21, pp. 435-454, 1992.
12. Leonard, B.P., A Stable and accurate Convective Modelling Procedure Based on Quadratic Upstream Interpolation, *Comp. Methods Appl. Mech. Engr.*, Vol. 19, pp. 59-98, 1979.

13. Mukhopadhyay, A., Biswas, G., and Sundararajan, T., Numerical Investigation of Confined Wakes behind a Square Cylinder in a Channel, *Int. J. Numer. Methods Fluids*, Vol. 14, pp. 1473-1484, 1992.
14. Okajima, A., Strouhal Numbers of Rectangular Cylinders, *J. Fluid Mech.*, Vol. 123, pp. 379-398, 1982.
15. Patankar, S.V., A Calculation Procedure for Two-Dimensional Elliptic Situations, *J. Numer. Heat Transfer*, Vol. 4, pp. 409-425, 1981.
16. Patankar, S.V., Numerical Heat Transfer and Fluid Flow, Hemisphere Publishing Co., 1980.
17. Patankar, S.V. and Spalding, D.B., A Calculation Procedure for the Heat, Mass and Momentum Transfer in Three-Dimensional Parabolic Flows, *Int. J. Heat and Mass Transfer*, Vol. 15, pp. 1787-1805, 1972.
18. Peyret, R. and Taylor, T.D., Computational Methods for Fluid Flow, Springer Verlag, 1983.
19. Robichaux, J., Tafti, D.K. and Vanka, S.P., Large Eddy Simulation of Turbulence on the CM-2, *J. Numer. Heat Transfer, Part-B*, Vol. 21, pp. 367-388, 1992.
20. Thomas, L.H., Elliptic Problems in Linear Difference Equation Over A Network, Waston Sci. Compt. Lab. Report, Columbia University, New York, 1949.
21. Van Doormal, J.P. and G. D. Raithby, G.D., Enhancement of the SIMPLE Methods for Predicting Incompressible Fluid Flows, *J. Numer. Heat Transfer*, Vol. 7, pp. 147-163, 1984.
22. Vanka, S.P., Chen, B. C. J. and Sha, W.T., A Semi-Implicit Calculation Procedure for Flows Described in Body-Fitted Coordinate System, *J. Numer. Heat Transfer*, Vol. 3, pp. 1-19, 1980.
23. Vieceilli, J.A., Computing Method for Incompressible flows Bounded by Moving Walls, *J. Comput. Phys.*, Vol. 8, pp. 119-143, 1971.

Problems

1. Develop the MAC and SIMPLE algorithms describes in this chapter for a steady one dimensional flow field $u(y)$, driven by a constant (but as yet undetermined) pressure gradient. For definiteness, flow in a parallel plate channel can be considered.
2. For a two-dimensional flow, show that the MAC type iterative correction of pressure and velocity field through the implicit continuity equation is equivalent to the solution of Poisson equation for pressure. How

does the procedure avoid the need of directly applying pressure-boundary-conditions?

3. Compare the solutions obtained by the stream function-vorticity method with those presented in this chapter for the following problems:
 - (a) Developing flow in a parallel plates channel;
 - (b) Flow past a square cylinder ($Re < 200$);
 - (c) Flow past a periodic array of square cylinders.
4. Apply MAC method to solve the shear driven cavity flow problem shown in Figure 6.13. Take a grid size of 51×51 and solve the flow equations for $Re = 400$.

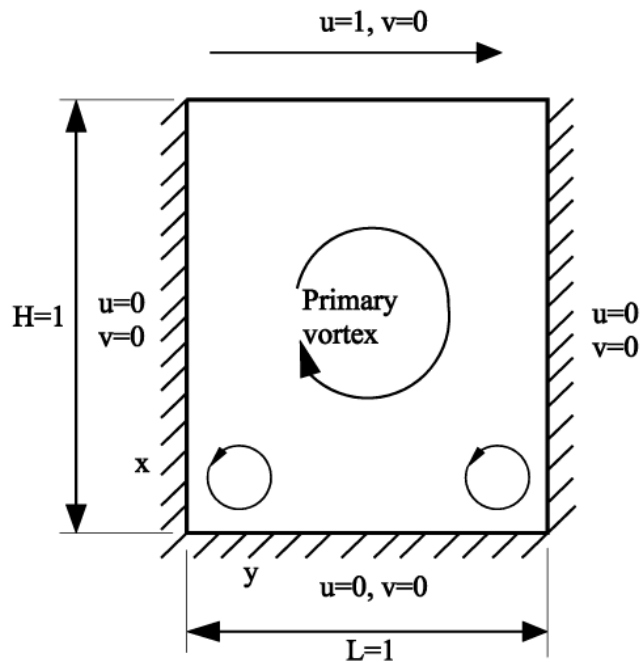


Figure 6.13: Shear driven Cavity

5. The Navier-Stokes equations in three-dimensional spherical-polar coordi-

nate system in θ direction may be written as

$$\begin{aligned} & \rho \left(\frac{\partial V_\theta}{\partial t} + V_r \frac{\partial V_\theta}{\partial r} + \frac{V_\theta}{r} \frac{\partial V_\theta}{\partial \theta} + \frac{V_\phi}{r \sin \theta} \cdot \frac{\partial V_\theta}{\partial \phi} + \frac{V_r V_\theta}{r} - \frac{V_\phi^2 \cot \theta}{r} \right) \\ = & - \frac{\partial p}{r \partial \theta} + \mu \left[\frac{\partial^2 V_\theta}{\partial r^2} + \frac{2}{r} \frac{\partial V_\theta}{\partial r} + \frac{1}{r^2} \frac{\partial V_\theta}{\partial \theta^2} + \frac{\cot \theta}{r^2} \frac{\partial V_\theta}{\partial \theta} \right. \\ & \left. + \frac{1}{r^2 \sin^2 \theta} \cdot \frac{\partial^2 V_\theta}{\partial \phi^2} + \frac{2}{r^2} \frac{\partial V_r}{\partial \theta} - \frac{V_\theta}{r^2 \sin^2 \theta} - \frac{2 \cot \theta \csc \theta}{r^2} \frac{\partial V_\theta}{\partial \phi} \right] \end{aligned}$$

The continuity equation is given by

$$\frac{\partial(\rho V_r)}{\partial r} + \frac{2}{r}(\rho V_r) + \frac{1}{r} \frac{\partial}{\partial \theta}(\rho V_\theta) + \frac{\cot \theta}{r} \rho V_\theta + \frac{1}{r \sin \theta} \frac{\partial}{\partial \phi}(\rho V_\phi) = 0$$

Discretize the weak conservative form of the θ -momentum equation on a grid (in spherical polar coordinate) using a weighted-average scheme.

6. Obtain the exact solution of the equation given by

$$\frac{d}{dx} \left(\rho u T - \Gamma \frac{\partial T}{\partial x} \right) = 0$$

where, ρu is the convective flux at the point u_{ij} has been defined (Figure 6.3) diffusion coefficient. Both ρu and Γ are constant over the control volume. The boundary conditions are: at $x = 0, T = T_P$ and at $x = \delta x_e, T = T_E$

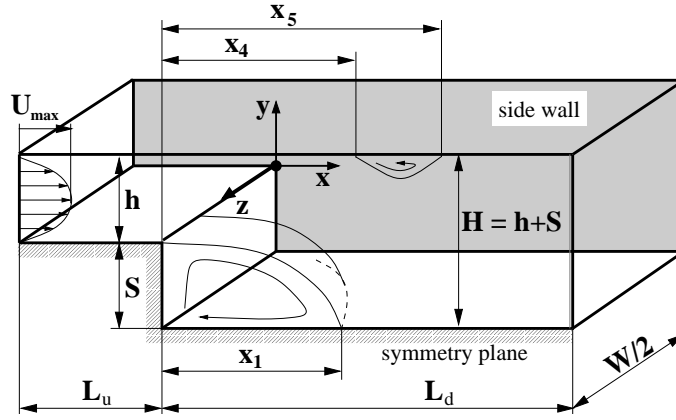


Figure 6.14: Flow over a Backward Facing Step

7. Solve three-dimensional Navier-Stokes equations for the flow over a backward facing step as illustrated in Figure 6.14. Find out the reattachment

length x_1 for the Reynolds numbers of 200, 300 and 400. The Reynolds number is given by $Re = \rho u(2h)/\nu$. Compare the results with that are available in Biswas et al. (2004)

8. Consider the channel flow and backward-facing-step configurations once again. Combine the flow and thermal energy equations and determine the local and global heat transfer rates when one of the solid surfaces is heated, the incoming fluid is cold and all other solid surfaces are thermally insulated.
9. Consider a square cylinder in a channel as shown in Figure 6.15.

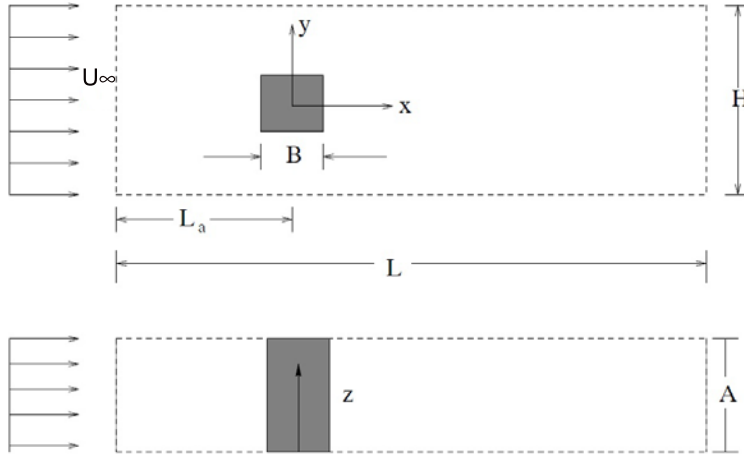


Figure 6.15: A square cylinder in a channel

For this assignment consider a 2D flow and neglect the dimensions in the z -direction.

Following are the relevant dimensions:

$$B = 1.0, H = 10.0, L_a = 7.5, L = 22.0.$$

The velocity profile is uniform at the inflow plane. Use 178 X 82 grids and solve complete Navier-Stokes equations on the 2D domain using SIMPLE/ MAC algorithm. The Reynolds number of interest is 40. Draw the streamlines and velocity vectors in the domain.

Having computed the velocity field, compute the temperature field using Successive Over Relaxation (SOR) scheme. The upper wall, lower wall

6.34 Computational Fluid Dynamics

and the obstacles are at temperature T_W . The incoming fluid is at a temperature T_∞ . Use smooth outflow boundary condition at the outflow plane. The Prandtl number of the fluid is 6.5. The temperature T_W may be assumed as 1.3 times T_∞ ; T_∞ being 300K.